

Mutagenesis of Transmembrane Domain 11 of P-Glycoprotein by Alanine Scanning[†]

Maya Hanna, Martine Brault, Tony Kwan, Christina Kast, and Philippe Gros*

Department of Biochemistry, McGill University, Montreal, Quebec, Canada H3G 1Y6

Received June 14, 1995; Revised Manuscript Received October 20, 1995[©]

ABSTRACT: The biochemical and genetic analyses of P-glycoprotein (P-gp) have indicated that the membrane-associated regions of P-gp play an important role in drug recognition and drug transport. Predicted transmembrane domain 11 (TM11) maps near a major drug binding site revealed by photoaffinity labeling, and mutations in this domain alter the substrate specificity of P-gp. To investigate further the role of TM11 in P-gp function in general, and substrate specificity in particular, each of the 21 residues of TM11 of the P-gp isoform encoded by the mouse *mdr3* gene was independently mutated to alanine, or to glycine in the case of endogenous alanines. After transfection and overexpression in Chinese hamster ovary cells, pools of stable transfectants were analyzed for qualitative or quantitative deviations from the profile of resistance to vinblastine, adriamycin, colchicine, and actinomycin D displayed by the wild-type protein. While mutations at eight of the positions had no effect on P-gp function, 13 mutants showed a 2–10-fold reduction of activity against one of the four drugs tested. Although the phenotype of individual mutants was varied, replacements at most mutation-sensitive positions seemed to affect the drug resistance profiles rather than the overall activity of the mutant P-gp. When TM11 was projected in a α -helical configuration, the distribution of deleterious and neutral mutations was not random but segregated with a more hydrophobic (mutation-insensitive) face and a more hydrophilic (mutation-sensitive) face of a putative amphipathic helix. The alternate clustering pattern of deleterious vs neutral mutations in TM11 together with the altered drug resistance profile of deleterious mutants suggest that the more hydrophilic face of the TM11 helix may play an important structural or functional role in drug recognition and transport by P-gp. Finally, the conservation of the two residues most sensitive to mutations (Y949 and F953) in TM11, and in the homologous TM5, of all mammalian P-gps and also in other ABC transporters, suggests that these residues and domains may play an important role in structural as well as mechanistic aspects common to this family of proteins.

Overexpression of P-glycoprotein (P-gp)¹ in cultured cells *in vitro* (Gottesman & Pastan, 1993) and in certain types of human tumors *in vivo* (Shustik *et al.*, 1995) causes the appearance of multidrug resistance (MDR). P-gp is a 170-kDa membrane glycoprotein that can bind photoactive analogs of cytotoxic drugs (Cornwell *et al.*, 1986; Safa *et al.*, 1986, 1989) and ATP (Cornwell *et al.*, 1987; Schurr *et al.*, 1989), shows ATPase activity [reviewed by Shapiro and Ling (1994)] and is believed to function as a drug efflux pump to reduce intracellular drug accumulation in resistant cells (Endicott & Ling, 1989; Gottesman & Pastan, 1993). P-gps are encoded by a small family of genes, with two members in humans (*MDR1* and *MDR2*) and three in rodents (*mdr1*, *mdr2*, and *mdr3*) that code for highly similar proteins sharing 78–91% sequence homology (Gros *et al.*, 1986, 1988; Devault & Gros, 1990; Chen *et al.*, 1986; van der Bliek *et al.*, 1988). P-gps are formed by two symmetrical halves,

each encoding six predicted transmembrane (TM) domains and one nucleotide binding (NB) domain (Gros *et al.*, 1986; Chen *et al.*, 1986). Transfection experiments in homologous (mammalian cells) or heterologous (yeast) expression systems have shown that human *MDR1* and mouse *mdr1/mdr3* cDNAs can confer drug resistance to drug-sensitive cells, while human *MDR2* and mouse *mdr2* cannot (Gros *et al.*, 1988; Schinkel *et al.*, 1991; Ruetz & Gros, 1994a). Recent experiments in mutant mice bearing a null allele at the *mdr3* locus have firmly established the role of this P-gp isoform in reducing drug accumulation in certain organs *in vivo*, most notably in the brain (Schinkel *et al.*, 1994). Although the exact mechanism by which P-gp transports drug molecules is not fully understood (Simon & Schindler, 1994), the liver-specific P-gp isoform encoded by mouse *mdr2* was recently demonstrated to function as a lipid flippase, translocating phosphatidylcholine molecules from the inner to the outer leaflet of the membrane lipid bilayer (Ruetz & Gros, 1994b; Smith *et al.*, 1994). P-gps are part of the superfamily of structurally related ATP binding cassette (ABC) membrane transporters, which includes members in prokaryotes (traffic ATPases of Gram-negative bacteria) and eukaryotes which act upon a vast group of unrelated substrates. ABC transporters include the human CFTR chloride channel and TAP-1/TAP-2 peptide transporters, the Pfmdr1 gene product of *Plasmodium falciparum* in which mutations are associated with chloroquine resistance, the yeast pheromone transporter

[†] This work was supported by a grant to P.G. from the Medical Research Council (MRC) of Canada. M.H. is supported by a fellowship PF-3780 from the American Cancer Society, T.K. by a studentship from the Cancer Research Society, and P.G. by a scholarship award from the MRC. P.G. is an International Research Scholar of the Howard Hughes Medical Institute.

* To whom correspondence should be addressed.

[©] Abstract published in *Advance ACS Abstracts*, February 15, 1996.

¹ Abbreviations: P-gp, P-glycoprotein; TM, transmembrane; MDR, multidrug resistance; CHO, Chinese hamster ovary; ACT, actinomycin D; ADR, adriamycin; COL, colchicine; VBL, vinblastine; WT, wild-type; amino acids are represented by their single-letter symbols.

STE6, and many others (Higgins, 1992). Structural similarity among these proteins must underlie conserved functional aspects of transport, as the mouse *mdr3* gene can complement STE6 and partially restore mating in a yeast *ste6* sterile mutant (Raymond *et al.*, 1992).

The capacity of P-gp to act on many structurally unrelated cytotoxic drugs that form the MDR group remains a puzzling aspect of P-gp function. Detailed structure/function studies aimed at identifying the P-gp domains and residues implicated in drug recognition and binding have identified the membrane-associated regions as playing a key role in this process. Indeed, energy transfer experiments with doxorubicin have indicated that hydrophobic drug molecules are probably recognized by P-gp within the context of the membrane bilayer (Raviv *et al.*, 1990). Furthermore, epitope mapping studies of P-gp proteolytic fragments photolabeled with azidopine or analogs of prazosin and forskolin identified membrane-associated regions as major sites for drug binding (Bruggemann *et al.*, 1989, 1992; Greenberger *et al.*, 1991; Greenberger, 1993; Morris *et al.*, 1991, 1994). Minor and major binding sites located in each half of P-gp have been delineated as two ≤ 5 -kDa proteolytic fragments symmetrically located near predicted TMs 6 and 12, respectively (Greenberger, 1993). Genetic analysis of chimeric molecules constructed between different members of the mouse or human P-gp family have also suggested that the membrane-associated regions are responsible for substrate specificity of individual P-gps (Buschman & Gros, 1991; Dhir & Gros, 1992; Zhang *et al.*, 1995). In addition, the study of naturally occurring human and hamster P-gp mutants with altered drug resistance profiles have indicated that discrete mutations near TM3 (G185V) or within TM6 (G338/A339 to A338/P339) alter substrate specificity of P-gp by modifying initial drug binding or drug release from the protein (Choi *et al.*, 1988; Safa *et al.*, 1990; Devine *et al.*, 1992). Finally, elegant studies of Loo and Clarke, in which proline and phenylalanine residues located within TM domains (Loo & Clarke, 1993a,b) as well as glycines in cytoplasmic loops of human MDR1 were systematically replaced by alanines (Loo & Clarke, 1994a), identified several residues within TM 4 (P223A), TM 6 (F335A), TM 10 (P866A), and TM 12 (F978A) and in the intervening cytoplasmic loops where mutations differentially affect the capacity of P-gp to confer resistance to vinblastine (VBL), adriamycin (ADR), colchicine (COL), and actinomycin D (ACT).

Studies from our laboratory have shown that independent mutations at serine 939 within the predicted TM11 of mouse Mdr1 and Mdr3 drastically affect (1) the activity (increase or decrease) of P-gp toward different drugs such as ADR, COL, VBL, and ACT (Gros *et al.*, 1991; Dhir *et al.*, 1993); (2) P-gp sensitivity to structurally distinct inhibitors (Kajiji *et al.*, 1994), and (3) its capacity to complement STE6 in yeast (Raymond *et al.*, 1992). Mutations at that site affect drug transport by modulating initial drug binding to the protein (Kajiji *et al.*, 1993), suggesting an important site for recognition of unrelated substrates and modulators. Since mutations at the homologous position of TM11 of *pfmdr1* are associated with altered function and chloroquine resistance in the malarial parasite (Foote *et al.*, 1990), and since TM11 maps very close to the major C-terminal drug photolabeling site of P-gp (Greenberger *et al.*, 1991; Greenberger, 1993; Morris *et al.*, 1994), we decided to further investigate the importance of this TM domain in the formation of a drug binding or transport site in P-gp. To

that end, we carried out a systematic mutagenesis of TM11, substituting one at a time each of 21 residues by an alanine (alanine scan). The effect of the alanine and glycine (in the case of wild-type alanines) substitutions on P-gp activity was assayed by ability of the mutant proteins to confer drug resistance to transfected Chinese hamster ovary (CHO) cells.

MATERIALS AND METHODS

Site-Directed Mutagenesis of the Mouse *mdr3* cDNA. A 1.7-kb *SmaI*–*PstI* fragment of *mdr3* cloned in the corresponding sites of M13mp19 polylinker served as the template for oligonucleotide site-directed mutagenesis using a commercially available kit (Amersham, Arlington Heights, IL). To facilitate subsequent transfer of the mutated cDNA fragments to a mammalian expression vector, *NruI* and *SpeI* restriction sites flanking TM11 on either side were first introduced by mutagenesis, using oligonucleotides (5′)-CTTCTGCTCGCGAGTCAA-(3′) [*NruI* site, position 2724 of the published sequence (Devault & Gros, 1990)] and (5′)-GAGAATACTAGTAGAACATTT-(3′) (*SpeI* site, position 2914). A novel *SalI* site was also introduced further N-terminal to TM11 at position 2480, using the oligonucleotide (5′)-CACAGCAAGTCGACTCCCTGTAGC-(3′). The nucleotide changes (indicated in bold letters) are silent and do not alter the amino acid sequence of P-gp. The integrity of the entire 1.7-kb *SmaI*–*PstI* fragment was verified by nucleotide sequencing, followed by reconstruction into the full-length *mdr3* cDNA in plasmid vector pGEM-7Zf (Promega). The resulting full-length *mdr3* cDNA (*mdr3.4*) was excised from this plasmid as a 4.1-kb *ClaI*–*SphI* fragment, and the ends were repaired with T4 DNA polymerase followed by cloning into the repaired *EcoRI* site of the mammalian expression vector pEMC2b (a gift from Dr. R. Kaufman, Yale University, New Haven, CT), creating pEMC2b-*mdr3.4*. This construct was subsequently used as the recipient for all mutations in the TM11 fragment. Individual amino acids in TM11 of *mdr3* were mutated to alanine or glycine (in the case of a wild-type alanine) using single-stranded M13mp19/*mdr3* DNA template and complementary mutagenic oligonucleotides shown in Figure 1. Following mutagenesis, the sequence of the *NruI*–*SpeI* cassette was determined for each mutant, followed by excision and reinsertion in the corresponding sites of pEMC2b-*mdr3.4*. Accessibility of the two cloning sites to restriction enzyme cleavage in these constructs was verified, and the presence of a single insert at these sites was monitored by digestion with *SalI* and *PstI*. Prior to transfection in CHO [LR73, Pollard and Stanners (1979)] cells, the presence of the correct mutations in the final constructs was verified once again by DNA sequencing. All nucleotide sequencing was by the dideoxy chain-termination method (Sanger *et al.*, 1977), using [³⁵S]α-dATP (New England Nuclear, specific activity 1348 Ci/mmol).

Cell Culture and DNA Transfections. pEMC2b-*mdr3.4* plasmids containing either wild-type (WT) or individual mutant *mdr3* cDNAs were introduced into LR73 cells by cotransfection with indicator plasmid pSV2neo (10:1 ratio) as calcium phosphate coprecipitates (Wigler *et al.*, 1979). Mass populations were selected in medium containing Geneticin (G418) at 1 mg/mL for a period of 11 days and were harvested as pools of 100–200 G418 resistant (G418^R) colonies. Subsequently, 2×10^6 G418^R cells from each pool

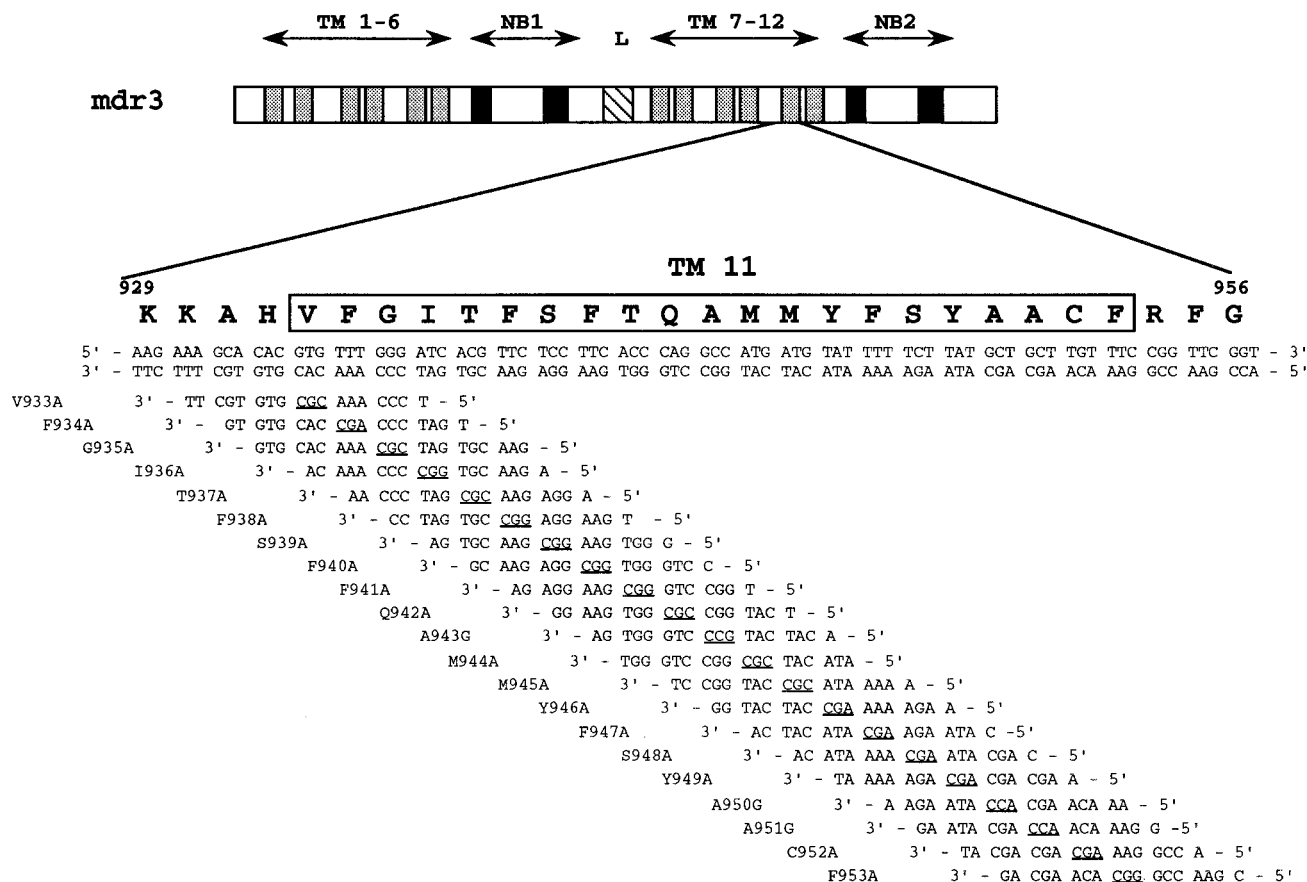


FIGURE 1: Site-directed mutagenesis of predicted TM11 of mouse Mdr3. A schematic representation of predicted structural domains of Mdr3 is shown at the top, including transmembrane domains (TM), nucleotide binding folds (NB1, NB2) and the linker region (L) which joins the two homologous halves of P-gp. The nucleotide and amino acid sequences (boxed) of TM11 between positions 929 and 956 are shown, as well as the sequences of the oligonucleotide primers used for site-directed mutagenesis. The mutagenized codons are underlined.

were plated in medium containing vinblastine at 25 ng/mL, and selection of vinblastine-resistant colonies (VBL^R) was allowed for a further 1–4 weeks. VBL^R cells were harvested as pools of 50–100 clones, expanded in culture, and frozen in 90% fetal calf serum (FCS) and 10% dimethyl sulfoxide as four separate aliquots. One aliquot of each was thawed out and used for each subsequent experiment. Minimum essential medium (α MEM) supplemented with 10% FCS, 2 mM glutamine, 50 units/mL penicillin, and 50 μ g/mL streptomycin was used in all experiments. Cell culture media, serum, growth supplements, and G418 were purchased from Gibco/BRL (Montreal, Canada).

Drug Survival Assay of VBL^R Mass Populations. A modification of a cell survival assay (Skehan *et al.*, 1989) based on sulforhodamine B (SRB) staining of total cell protein was used (Tang-Wai *et al.*, 1993). Briefly, 5×10^3 cells from VBL^R mass populations of either control or *mdr3* cotransfected cells were plated in 96-well titer plates in medium containing increasing concentrations of vinblastine (VBL), colchicine (COL), adriamycin (ADR), or actinomycin D (ACT) and incubated for 72 h at 37 °C. Cells were then washed once in ice-cold PBS, fixed in 17% trichloroacetic acid in PBS for 1 h at 4 °C, and then washed extensively in tap water. Cellular proteins were stained with a solution of 0.4% SRB in 1% acetic acid for 15 min at room temperature, followed by four washes with 1% acetic acid to remove excess stain. After the plates were dried, the stain was dissolved in 10 mM Tris (pH 9.0), and quantification was carried out using an automated ELISA plate reader (Bio-Rad Model 450) set at 490 nm. The relative plating efficiency of each mass population was calculated by

dividing the absorbance observed at a given drug concentration by the absorbance detected in the same population in medium devoid of drug and is expressed as a percentage. D_{50} is defined as the drug dose required to reduce plating efficiency of each transfected cell population by 50% and is an average from three independent experiments.

Drug Survival Assay of G418^R Mass Populations. Untransfected LR73 cells and G418^R mass populations of LR73 transfected with WT and I936A, Q942A, Y949A, and F953A mutant *mdr3* cDNAs were plated in medium without drug (2.5×10^3 cells) or in medium containing ACT, ADR, COL, or VBL at three different concentrations (2.5×10^4 cells) in 24-well plates (15-mm wells). Plates were incubated for 7 days at 37 °C with one change of medium after 3 days. Cells were washed once with warm PBS, fixed in 3.7% formaldehyde, and stained with crystal violet (1% in 20% ethanol) for 15 min. Excess stain was removed with five washes in water, and the plates were dried and photographed.

Membrane Preparations and Immunoblotting. Crude membrane extracts from cultured cells were prepared by homogenizing cells in hypotonic buffer as previously described (Schurr *et al.*, 1989). Protein concentration was determined using a Coomassie blue-based commercial assay (Bio-Rad). Sodium dodecyl sulfate–polyacrylamide gel electrophoresis (SDS–PAGE) was performed according to standard protocols (Laemmli, 1970). Briefly, 3 μ g of membrane proteins were solubilized in 2 \times Laemmli sample buffer for 30 min at room temperature before being loaded onto 7.5% polyacrylamide gels. After electrophoresis, gels were equilibrated in transfer buffer (20% methanol, 0.76 M

glycine, and 2.5 mM Tris, pH 8) and proteins were transferred to nitrocellulose sheets by Western blotting (0.5 A at 100 V, at 4 °C) for 1 h. The blots were treated to prevent nonspecific binding by incubation overnight at 4 °C in TBST (10 mM Tris, pH 8, 0.15 M NaCl, and 0.02% Tween 20) and 1% BSA, followed by incubation with a 1:300 dilution of mouse anti-P-gp monoclonal antibody C219 (Centocor) (Kartner *et al.*, 1985) for 1 h at room temperature, and then with goat anti-mouse antibody conjugated to alkaline phosphatase. Specific antigen–antibody complexes were revealed by incubation with 5-bromo-4-chloro-3-indoyl phosphate *p*-toluidine and nitroblue tetrazolium (Gibco/BRL).

Immunofluorescence. Mass populations of VBL^R cells expressing either the wild-type Mdr3 protein or the F953A mutant were analyzed for cellular and subcellular distribution of P-gp by immunofluorescence. The cells were fixed in 4% paraformaldehyde in PBS and permeabilized and blocked with 0.05% Nonidet-P40 in PBS, 5% goat serum, and 1% bovine serum albumin at room temperature for 15 min. The cells were then incubated with the isoform-specific rabbit anti-mouse Mdr3 antibody B2037 (Devault & Gros, 1990), used at 1:500 dilution. The cells were then washed with PBS, followed by incubation with a secondary antibody (rhodamine-conjugated goat and anti-rabbit IgG antibody; Jackson ImmunoResearch Laboratories, Inc., West Grove, PA), used at 1:100 dilution. Immunofluorescence microscopy was performed using standard epifluorescence optics (Zeiss Axiophot).

Expression and Testing of Mdr3 Function in Yeast Cells. *Saccharomyces cerevisiae* strains JPY201 (McGrath & Varshavsky, 1989) was used to test the biological activity of wild-type *mdr3* and the F953A mutant (drug resistance). JPY201 cells were transformed by the lithium acetate method (Ito *et al.*, 1983), with a yeast expression vector (pVT) that we have previously described (Raymond *et al.*, 1992) and that contained either the wild-type *mdr3* cDNA (pVT-*mdr3*) or the F953A mutant, and pools of *ura*⁺ colonies were harvested, expanded in culture, and kept frozen until use in each experiment. Cellular resistance of yeast transformants expression either wild-type *mdr3* or mutant F953A cDNAs was estimated by a growth inhibition assay in liquid culture using the antifungal macrolite peptide FK506 and valinomycin, previously shown to be P-glycoprotein substrates in yeast (Raymond *et al.*, 1994; Kuchler & Thorner, 1992). The growth inhibition assay was carried out essentially as described (Raymond *et al.*, 1994). Briefly, fresh overnight cultures of *mdr3* transformants grown in SD-*ura* were diluted to OD 0.005 (600 nm) in YPD medium and added (50 μ L) to an equal volume of YPD medium containing FK506 or valinomycin (both at 50 μ g/mL) in a 96-well microwell titer plate. The plates were wrapped with Parafilm to prevent evaporation and incubated at 30 °C with constant agitation (250 rpm), and growth was monitored by optical density measurement using an ELISA plate reader (Bio-Rad, Model 450) set at 490 nm.

Computer-Assisted Sequence Analyses. Analyses of predicted amino acid sequences of ABC transporters were performed on the VAX/VMS server at the Université de Montréal using the GCG software package and were aligned with the Pileup program (Devereux, 1991). A helical wheel projection of the primary amino acid sequence of TM11 was constructed, using 3.6 amino acids per turn of the helix, as previously described (Gros *et al.*, 1991).

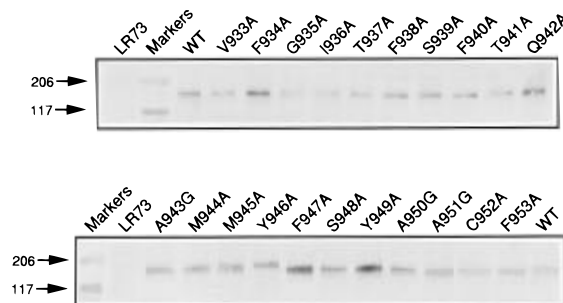


FIGURE 2: Detection of wild-type and mutant P-gps in membrane fractions from VBL^R mass populations of stably transfected cells. Three micrograms of proteins from crude membrane preparations from control untransfected cells (LR73) or from cells transfected with either wild-type *mdr3* (WT) or individual mutants (as indicated) was loaded in each lane and transferred to nitrocellulose membranes. Blots were incubated with anti-P-gp monoclonal antibody C219 to reveal the presence of P-gps of apparent molecular mass 170 kDa. Prestained molecular mass markers are myosin (206 kDa) and β -galactosidase (117 kDa).

RESULTS

Construction and Expression of TM11 *mdr3* Mutants in CHO Cells. Previous studies from our group of *mdr3* mutants bearing single amino acid substitutions at serine position 939 in predicted TM11 of P-gp suggested that this residue and membrane domain may be implicated in the formation of a drug binding site (Gros *et al.*, 1991; Dhiri *et al.*, 1993; Kajiji *et al.*, 1993, 1994). To further test this possibility, and to identify additional amino acid residues implicated in this process, we carried out a systematic mutagenesis of all residues predicted to form TM11 using an alanine scan approach. In this scheme, each residue was individually substituted by an alanine. Alanine's small size, neutral side group, strong helical propensity, and prevalence in all types of secondary structure domains, in both buried and exposed surfaces, make it a structurally neutral substitution, which is most likely to show the consequences of loss of information without introducing new spatial or electrostatic constraints. The three existing alanines in TM11 were replaced by glycines, in order to avoid the introduction of a new side chain. Individual substitutions were introduced into TM11 by site-directed mutagenesis in M13mp19, using oligonucleotides listed in Figure 1, and transferred into the full-length *mdr3* cloned in the mammalian expression vector pEMC2b. Constructs bearing WT or mutant *mdr3* cDNAs were introduced in drug-sensitive LR73 cells by cotransfection with the indicator plasmid pSV2neo (Southern & Berg, 1982), followed by selection of G418^R colonies in medium containing G418, which were then harvested as mass populations. To test the ability of mutant *mdr3* cDNAs to confer drug resistance, these G418^R mass populations were directly plated in medium containing a low concentration (25 ng/mL) of the cytotoxic drug VBL. Mass population of G418^R cells harboring either wild-type or mutant *mdr3* cDNAs yielded VBL^R colonies within a week of drug selection, except for the C952A and Y946A mutants, which grew more slowly and required growth periods of 2 and 4 weeks, respectively, in order to reach the confluency obtained for the WT and other *mdr3* mutants (data not shown). These mass populations of VBL^R clones were harvested as pools and expanded in culture, and membrane fractions were prepared from these cells and analyzed by immunoblotting for the presence of corresponding Mdr3 proteins using the anti-P-gp monoclonal antibody C219 (Figure 2). These

experiments demonstrated the presence of a specific immunoreactive band of approximately 170 kDa in VBL^R mass populations isolated from all *mdr3* mutants and which was absent from control untransfected LR73 cells. The level of expression of the mutant proteins in these populations was very similar but not identical; in addition, we noted small differences in electrophoretic mobility and proportion of glycosylated isoforms of the various P-gp mutants. However, no specific correlations between these variations and the phenotypes of the various mutants were evident (see below). These experiments suggest that the various mutations introduced in TM11 did not abrogate function, since the corresponding mutant P-gps appear capable of conferring resistance to VBL and did not drastically impair membrane targeting, since mutant P-gps were found present in the cell membrane fractions.

Individual Mutations in TM11 Affect Overall Activity and Substrate Specificity of P-gp. The capacity of mass populations of cotransfectants expressing individual TM11 mutants to grow in low concentrations of VBL (previous section) indicated that none of the mutations completely abolished *mdr3* function. Since we have previously observed that individual mutations at S939 (within TM11) affect substrate specificity of *mdr3* and *mdr1* (Gros *et al.*, 1991; Dhir *et al.*, 1993), we determined if any of the TM11 mutations had a qualitative or quantitative effect on the degree of resistance conferred by the corresponding P-gps to different classes of MDR drugs, namely, VBL, COL, ADR, and ACT. For this, the dose required to reduce the plating efficiency of each mass population of VBL^R cells by 50% was calculated for the four drugs and is presented as a D_{50} in Figure 3 and as a resistance index (fold resistance) in Table 1. Results from these experiments indicated that individual mutations in TM11 could affect either the overall activity or the specificity of mutant P-gps for the four drugs tested. On the basis of the magnitude of the deleterious effect on P-gp activity against one or more drugs, individual mutants could be classified into three groups. Eight of the mutations (V933A, T937A, F940A, M944A, M945A, F947A, A950G, and A951G) had no significant effect on function, and the corresponding mutant P-gps expressed levels of resistance to each drug similar to that of WT. Eleven of the mutations (F934A, G935A, I936A, F938A, S939A, T941A, Q942A, A943G, Y946A, S948A, and C952A) caused a moderate but reproducible 2–3-fold decrease in resistance to one or more of the drugs. Finally, two mutations, Y949A and F953A, caused a more dramatic 5–10-fold loss of resistance to one or more drugs tested. Among mutants with reduced activity, only F953A and I936A displayed an overall decrease in resistance to all drugs analyzed. On the other hand, most other deleterious mutations seemed to affect resistance only to one or two of the four drugs tested. For example, mutants S939A and Q942A showed wild-type activity against VBL and ACT but had reduced activity against ADR and COL, while mutant A943G displayed reduced activity only against ADR, and mutant Y949A had wild-type activity only against VBL. Overall, these results indicate that mutations in Mdr3 TM11, at residues other than S939, can also modulate substrate specificity of P-gp, suggesting that this domain and the identified residues may participate in the formation of, or be located near, a drug binding site.

Distribution of Mutation-Sensitive Residues in TM11. Analyzing the distribution of mutation-sensitive residues along the linear sequence of the proposed TM11 failed to

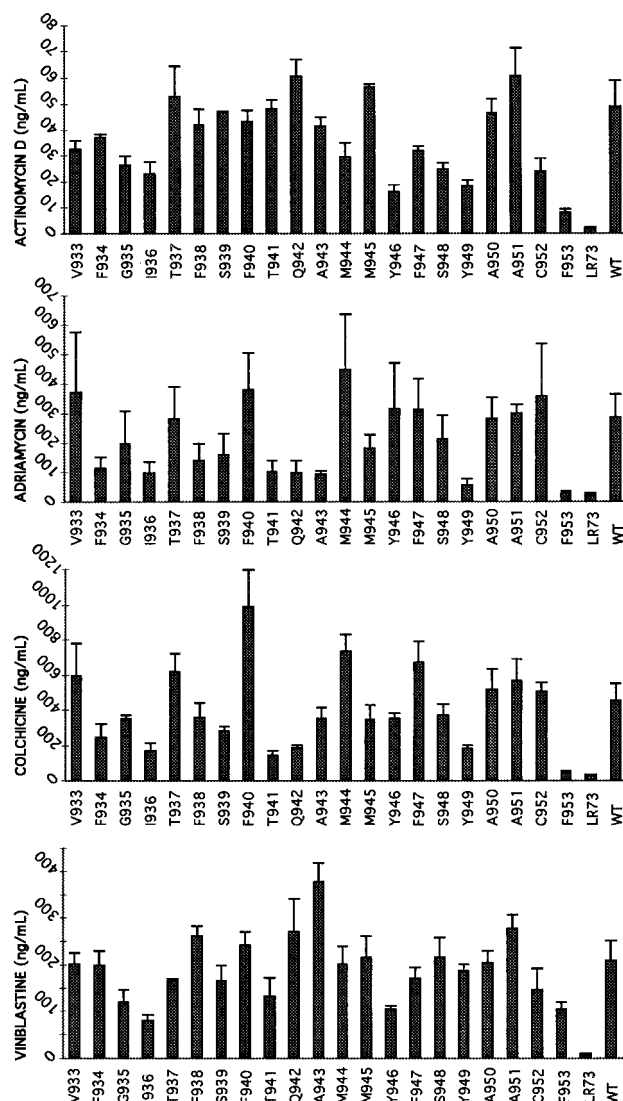


FIGURE 3: Multidrug resistance profiles of mass population LR73 cells transfected with either WT or mutant *mdr3* cDNAs. D_{50} s (in nanograms per milliliter, mean of three independent experiments) for the drugs actinomycin D, adriamycin, colchicine, and vinblastine were determined as described in Materials and Methods and are presented as histograms with the corresponding standard deviations. Shown are control untransfected cells (LR73) and cell populations transfected with either wild-type *mdr3* (WT) or mutant *mdr3* cDNAs bearing single mutations at the indicated position. Residues (other than alanines) were mutated to alanine. Alanines were mutated to glycines.

identify any subregion of this domain particularly sensitive or insensitive to amino acid substitutions. However, when this TM domain was looked at in a helical wheel projection, a nonrandom distribution of deleterious and neutral mutations was readily apparent (Figure 4). On a helical wheel projection, TM11 shows a highly hydrophobic face and a more hydrophilic one, which includes two serines, two threonines, a glutamine, and two tyrosines. Strikingly, seven of the eight mutations which were without consequences on *mdr3* function map to the highly hydrophobic face of this helix, with six of them (V933A, T937A, F940A, M944A, F947A, and A951G) clustered in a continuous mutation-insensitive segment (Figure 4). Included in this group are two nonconservative substitutions, F940A and F947A, in which a large aromatic side chain is replaced by a methyl group, and the T937A mutant, in which a hydrophilic hydroxyl group is eliminated. Also in this group, were two of the three Ala to Gly substitutions (A950G and A951G)

Table 1: Drug Survival Characteristics of Mass Populations Cells Stably Transfected with Wild-Type or Mutant *mdr3* cDNAs^a

<i>mdr3</i>	ACT	ADR	COL	VBL
V933A	32 ± 3 (17×)	370 ± 200 (19×)	590 ± 180 (21×)	200 ± 20 (24×)
F934A	37 ± 2 (19×)	110 ± 40 (6×)	240 ± 80 (9×)	200 ± 30 (24×)
G935A	26 ± 3 (14×)	200 ± 110 (10×)	350 ± 20 (13×)	120 ± 20 (14×)
I936A	23 ± 5 (12×)	100 ± 40 (5×)	170 ± 40 (6×)	80 ± 13 (10×)
T937A	50 ± 10 (27×)	280 ± 110 (15×)	620 ± 100 (23×)	160 ± 6 (20×)
F938A	42 ± 6 (22×)	140 ± 60 (7×)	360 ± 80 (13×)	260 ± 20 (32×)
S939A	46 ± 1 (24×)	160 ± 80 (8×)	280 ± 30 (10×)	160 ± 30 (20×)
F940A	43 ± 4 (22×)	380 ± 130 (20×)	980 ± 210 (36×)	240 ± 30 (29×)
T941A	48 ± 3 (25×)	100 ± 40 (5×)	140 ± 20 (5×)	130 ± 40 (16×)
Q942A	60 ± 6 (32×)	100 ± 40 (5×)	190 ± 10 (7×)	270 ± 70 (33×)
A943G	41 ± 4 (22×)	90 ± 10 (5×)	350 ± 60 (13×)	380 ± 40 (46×)
M944A	29 ± 6 (15×)	450 ± 190 (23×)	730 ± 90 (27×)	200 ± 40 (24×)
M945A	56 ± 2 (29×)	180 ± 50 (9×)	340 ± 80 (13×)	210 ± 50 (26×)
Y946A	16 ± 2 (8×)	310 ± 160 (16×)	350 ± 30 (13×)	100 ± 8 (13×)
F947A	32 ± 2 (17×)	310 ± 100 (16×)	660 ± 120 (24×)	170 ± 30 (20×)
S948A	25 ± 3 (13×)	210 ± 80 (11×)	370 ± 60 (13×)	210 ± 40 (26×)
Y949A	18 ± 2 (9×)	60 ± 20 (3×)	180 ± 20 (6×)	190 ± 15 (23×)
A950G	46 ± 6 (24×)	280 ± 70 (15×)	520 ± 120 (19×)	200 ± 30 (25×)
A951G	60 ± 10 (32×)	300 ± 30 (16×)	560 ± 120 (21×)	280 ± 30 (34×)
C952A	24 ± 5 (12×)	360 ± 180 (19×)	500 ± 50 (18×)	140 ± 50 (18×)
F953A	8 ± 1 (4×)	28 ± 7 (1×)	45 ± 9 (2×)	100 ± 13 (13×)
WT	50 ± 10 (25×)	290 ± 80 (15×)	450 ± 100 (16×)	210 ± 40 (25×)
LR73	2 ± 0.1 (1×)	19 ± 6 (1×)	27 ± 4 (1×)	8 ± 2 (1×)

^a The drug survival of Chinese hamster ovary drug-sensitive cells (LR73) and of cell clones transfected with either wild-type or mutant *mdr3* is expressed as the D_{50} (in nanograms per milliliter), or the dose necessary to reduce the plating efficiency of the control and transfected cells by 50%. The resistance index is the degree of resistance above background levels expressed in LR73 cells and is shown in parentheses.

933-V F G H I T F S F T Q A M M Y F S Y A A C F 953

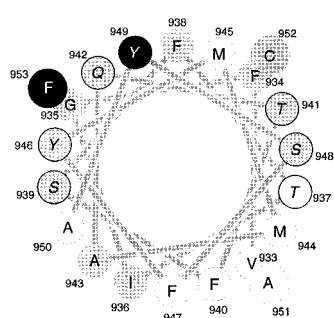


FIGURE 4: Position of mutation-sensitive and mutation-insensitive residues in predicted TM11 of Mdr3. The amino acid sequence of TM11 of Mdr3 is shown on top and the helical wheel projection of this domain is shown below. The helical wheel is viewed from its C-terminus with the last three residues (A951, C952, F953) offset to the outside. Residues with hydrophilic side chains are indicated in italics and with a black frame (top) or circle (bottom). Residues insensitive to mutation have a white background, moderately affected residues (2–3× reduction in activity) have a gray background, and severely affected residues (5–10× reduction) are shown with white letters on a black background.

introduced in TM11, indicating no ill effect on the structure or function of TM11 from the new potential for a tighter helical turn or greater rotational flexibility of the main chain by introduction of glycines at these positions. Substitutions near or at the proposed border of the hydrophobic and more hydrophilic faces of the domain did not dramatically affect Mdr3 activity; elimination of the hydroxyl groups at positions T937A, S939A, and S948A either had no effect (T937A) or caused only a small reduction (S939A and S948A; up to 2× reduction) in the activity of the mutant proteins. This suggests that the precise location of the polar/hydrophobic boundaries of TM11 is not critical for the drug resistance activity of P-gp, and its alteration causes no significant structural shifting. Among the amino acids on the more hydrophobic side of the helix, I936A showed the greatest sensitivity to alanine substitution, resulting in an overall 2–3-

fold reduction in activity against the four drugs tested. The somewhat lower level of expression of the I936A mutant in the membrane fraction of transfectants might have partly contributed to the reduced activity of this mutant. Similarly, a lower expression level of the G935A mutant may have contributed to its reduced overall activity. Nevertheless, these results together indicate that the majority of TM11 mutations that were without effect on Mdr3 function clustered on one side of an α -helical projection of this domain.

Conversely, the two mutations that had the most dramatic deleterious effect on Mdr3 function were found to map on the opposite and less hydrophobic side of the α -helical projection for TM11. Indeed, the F953A mutant, although retaining 50% of the wild-type activity for VBL, has lost most if not all activity against ADR, COL, and ACT (Figure 3). The level of expression of F953A in the membrane of stable transfectants (Figure 2) cannot account for the severe reduction in its ability to confer drug resistance. To further analyze the cellular expression and subcellular distribution of the F953A mutant, we used immunofluorescence with a rabbit isoform-specific anti-mouse Mdr3 antibody (B2037; Devault & Gros, 1990) to compare the pattern of expression of wild-type Mdr3 and F953A in stably transfected CHO cells expressing each protein. Results in Figure 5 indicate similar levels of expression of wild type (panel 2) and F953A (panel 3) mutants in these cells, with a ringlike staining at the periphery of the cells, typical of membrane-associated expression of both proteins. Likewise, the Y949A substitution caused the second-most severe loss of function, resulting in almost complete loss of ADR resistance and 2.5–3× loss of resistance to ACT and COL, while VBL resistance was unaffected in this mutant. On a helical wheel projection the F953A and Y949A mutations map very close to each other and symmetrically opposite to the cluster of neutral mutations mapping to the other, more hydrophobic face of TM11 (Figure 4). These two mutations are also predicted to map near the top half of TM11, within the outer lipid leaflet of

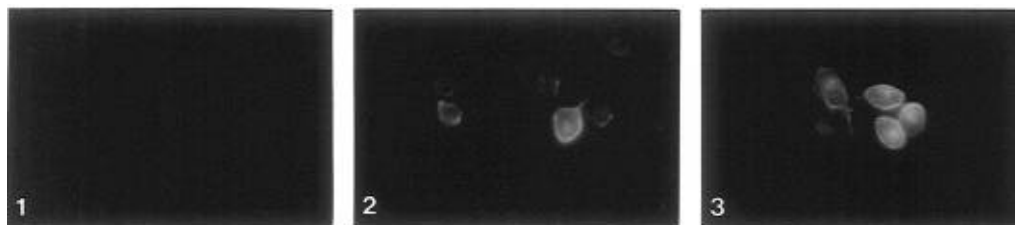


FIGURE 5: Immunofluorescence analysis of wild-type Mdr3 and F953A Mdr3 mutant in transfected CHO cells. Control LR73 cells (1) and transfectants stably expressing either wild-type Mdr3 (2) or the F953A Mdr3 mutant (3) were exposed to the rabbit anti-mouse Mdr3 isoform-specific antibody B2037 (Devault & Gros, 1990). Cells were then incubated with a second goat anti-rabbit antibody conjugated to rhodamine, and the cells were photographed using a fluorescence microscope.

the membrane bilayer. It is interesting to note that replacements at residues which neighbor F953 and Y949 on the helical projection and within the outer leaflet also had significant although less dramatic effects on Mdr3 activity: The Q942A mutation (positioned between Y949 and F953) caused 3 \times and 2 \times loss of resistance to ADR and COL, respectively, while the Y946A mutation (next to F953) caused a 3 \times and 2 \times decrease in resistance to ACT and VBL, respectively. On the other hand, the G935A substitution predicted to be positioned directly below F953 at the other end of TM11, in the inner leaflet of the membrane, did not alter Mdr3 function significantly. Taken together, these results indicate that a group of deleterious mutations, including the two most severe ones, map together on the more hydrophilic face of the TM11 helix, and directly opposite to a cluster of neutral mutations on the more hydrophobic face of TM11.

Although not perfectly segregated, the alternate clustering pattern of deleterious vs neutral mutations in TM11 suggests that the more hydrophilic face of the helix may play an important structural or functional role in drug recognition and transport by P-gp.

DISCUSSION

Identifying the P-gp segments and amino acid residues implicated in substrate interaction would shed light on the mechanism of action of this protein and may also help in the molecular modeling of new cytotoxic drugs or modulators capable of bypassing or blocking P-gp activity, respectively. In the absence of high-resolution three-dimensional structure information for P-gp, the identification of such determinants has relied on classical biochemical and genetic analyses. The characterization of P-gp peptide fragments photolabeled with drug analogs has indicated that the membrane-associated regions of both P-gp halves (TM5–6 and TM11–12) participate in drug binding. Likewise, experiments with chimeric and mutant proteins showed that mutations of certain residues within specific TM domains affect the substrate specificity of P-gp by modulating the transport, initial binding, or release of certain of its substrates (reviewed in the introduction). One residue of mouse Mdr1 and Mdr3 P-gps, in which mutations affect drug specificity, binding, and transport, is S939 situated within TM11 (Gros *et al.*, 1991; Dhir *et al.*, 1993; Ruetz *et al.*, 1993; Ruetz & Gros, 1994a; Kajiji *et al.*, 1993). Interestingly, of all the putative TM domains of Mdr3, TM11 shows the strongest amphipathic character (segregation of a hydrophobic and more hydrophilic faces), with S939 mapping at the boundary of the two faces of the putative helix (Gros *et al.*, 1991). To further probe the contribution of TM11 in general, and its amphipathic character, in particular, to the formation of a

possible substrate binding site, we have systematically mutated each residue of this domain to alanine. Alanine is structurally neutral and does not introduce new steric or electrostatic constraints on the peptide backbone. A similar alanine scan procedure has recently been used to identify important residues in TM6 of P-gp (Loo & Clarke, 1994b).

Results from these experiments indicated that all residues of this segment could be mutated without a complete loss of activity of the resulting proteins, since all mutants retained VBL resistance. However, mutations at several positions caused either a partial or, in certain cases, a complete loss of resistance to certain drugs, such as ADR and COL. These observations confirm and extend our previous observations obtained with a series of mutations at S939 and suggest that several residues in TM11 may interact directly or indirectly with some P-gp substrates. We observed that more than one-third of the residues could be replaced without significant loss of P-gp activity. Examination of the positioning of mutation-sensitive and insensitive residues on a helical wheel projection of TM11 showed a nonrandom distribution. We observed a clustering of mutation-insensitive residues to one side of the helix (apolar hydrophobic side), and the juxtaposition of several, including the two most highly sensitive residues (Y949 and F953), directly opposite, in the more polar face of the helix. Mutations at residues forming the polar/apolar boundary (T937 and S939) did not affect P-gp activity. Thus, although the exact location of the polar/apolar boundary does not appear critical for function, the apparent segregation of mutation-sensitive and insensitive residues suggests that the putative amphipathic character of TM11 is an important structural/functional feature of this domain.

We noted that the altered profile of drug resistance expressed by several of the TM11 mutants followed a similar trend: while many mutations caused a strong modulation of COL and ADR resistance, the mutant proteins retained fairly normal levels of VBL resistance (Figure 3). We tested the possibility that the VBL preselection procedure used in our study to obtain cell populations overproducing individual mutants may unduly affect the phenotype of these cells, possibly accounting for the apparent lack of effect of mutations on VBL resistance. For this, mass populations of G418^R cells cotransfected with individual mutants I936A, Q942A, Y949A, and F953A, showing unique deviations from wild type in their drug resistance profiles (Figure 3), were plated directly in medium containing increasing concentrations of VBL, ADR, COL, and ACT. The plates were incubated for 7 days, fixed, and then stained for cell survival (Figure 6). In addition, the amount of cell-associated protein was further quantitated by a standard protein assay, and the drug cytotoxicity for each cell population (expressed as the D_{50}) and the relative level of resistance (expressed as the

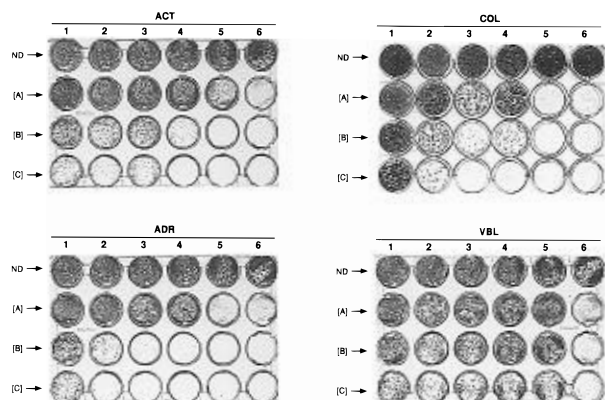


FIGURE 6: Drug survival characteristics of G418^R mass populations of transfected cells before preselection in vinblastine. Approximately 2.5×10^3 cells (no drug) or 2.5×10^4 cells (with drug) from mass populations of G418^R clones stably transfected with either wild-type *mdr3* (columns 1) or *mdr3* mutants I936A (2), Q942A (3), Y949A (4), F953A (5), or untransfected LR73 control cells (6) were plated in medium containing increasing concentrations of the drugs actinomycin D (ACT), adriamycin (ADM), colchicine (COL), or vinblastine (VBL). ND, no drug. Concentrations [A], [B], and [C] are 10, 25, and 50 ng/mL for ACT; 30, 100, and 200 ng/mL for ADM; 100, 250, and 500 ng/mL for COL; and 50, 100, and 200 ng/mL for VBL, respectively. Plates were incubated for 7 days, stained, and photographed.

Table 2: Drug Survival Characteristics of Mass Populations of G418^R Cell Clones Transfected with Mouse *mdr3* mutants in TM11^a

	ACT	ADM	COL	VBL
REV	7.5	52.6	71.9	8.0
I936A	59.7 (8.0×)	121.3 (2.3×)	367.1 (5.1×)	70.5 (8.8×)
Q942A	54.1 (7.2×)	82.6 (1.6×)	128.1 (1.8×)	81.7 (10.2×)
Y949A	31.6 (4.2×)	80.4 (1.5×)	163.3 (2.3×)	81.0 (10.1×)
F953A	9.4 (1.2×)	51.6 (1×)	85.9 (1.2×)	78.9 (9.9×)
WT	67.2 (9.0×)	249.4 (4.7×)	493.7 (6.9×)	67.6 (8.5×)

^a The drug cytotoxicity for each mass population of G418^R cell clones is expressed as the D_{50} (nanograms per milliliter), or the dose necessary to reduce the plating efficiency of the control and transfected cell clones by 50%. The relative degree of drug resistance, expressed as fold resistance over background levels detected in control mass populations transfected with the wild-type *mdr3* cDNA in the antisense orientation (REV), is shown in parentheses. ACT, actinomycin; ADM adriamycin; COL, colchicine; VBL vinblastine.

fold resistance) were calculated and are shown in Table 2. Drug resistance profiles of the mutants, as measured on G418^R mass populations by these assay, were strikingly similar to the drug resistance profiles of VBL-preselected cells shown in Figure 3. These results are in agreement with similar control experiments carried out previously with a series of mutants at S939 (Gros *et al.*, 1991) and indicate that the preselection in a low concentration of VBL has no effect on the drug resistance profile of individual mutants.

In the sequence alignment presented in Figure 7, we have analyzed the degree of conservation of mutation-sensitive residues in TM11 of all P-glycoproteins sequenced to date, as well as in the same region of other ABC transporters which share sequence homology and structural similarity to P-gp. Also, since many ABC transporters are formed by two sequence-homologous and symmetrical halves, we have included in the alignment the corresponding sequences of TM5 from all P-gps and some of the other ABC transporters for possible conservation or divergence at these positions. Of the 21 amino acid residues forming TM5 and TM11 of the P-gp family from rodents and man, we found six amino acids to be invariant at the homologous positions of the two

TM domains. Mutations at residues Y949 and F953 had the most drastic effect on P-gp activity, causing a 5–10-fold reduction in resistance to certain drugs (ADR and COL). These two residues were found to be precisely conserved in both TM11 and TM5 of all P-gps sequenced to date. F953, which suffered the most drastic loss of activity, is the most highly conserved one, also appearing in TM5 and/or TM11 of other ABC transporters from worm, fly, yeast, and protozoa (CepgpA,C; Mdr65; Ste6; Hst; and Pfmdr1, respectively), as well as in human Cftr and its homologs from mouse, frog, and dogfish. In the case of Y949, it is conserved in TM5 and 11 of all P-gps, and in addition, in TM11 of the *Drosophila* and *Arabidopsis* P-gp homologs, but it is not preserved in the CFTR family. Additional mutations at this position indicated that the effect of the mutation was not linked to the loss of the bulky side chain of the tyrosine residue but may involve specific chemical properties of this residue. Indeed, we observed that Y949F had characteristics very similar to Y949A, while Y949Q was near wild type with only a 2-fold reduction observed for adriamycin resistance (data not shown). Another mutation-sensitive position, I936, was also found to be highly conserved in the P-gp family and in certain ABC transporters. As opposed to other mutation-sensitive positions, the I936A mutation caused an overall reduction by a factor of 2–3-fold in activity of the mutant P-gp, reduction which could not be totally explained by a lower amount of protein produced in the clone analyzed (compare expression and activity to that of G935A). I936 is found in all TM5 and TM11 sequences of all eight rodent and human P-gps and is also found in either TM5 or TM11 of yeast and *Caenorhabditis elegans* homologs. In addition, an isoleucine or the closely conserved leucine are also found at that position in four examples of prokaryotic ABC transporters. The conservation at these residues in the P-gp families and in other ABC transporters together with their sensitivity to alanine replacement suggest that they may play a key role in structural or functional aspects common to this group of proteins.

The nonrandom distribution of mutation sensitive- and mutation-insensitive residues within predicted TM11 suggests that the apparent amphipathic character of this domain is important in the structural/functional integrity of P-gp. Indeed, while the most hydrophobic face of this helix seemed relatively insensitive to alanine replacements, the more hydrophilic one contained several residues that could not be substituted to alanine without affecting the activity of the protein. In addition, the observation that mutations at these sites generally affect substrate specificity rather than overall activity suggests that these residues and this portion of this TM domain may be important for recognition/transport of certain P-gp substrates (COL and ADR). Another interesting feature of TM11 is that it displays periodicity in its sequence conservation among members of the MDR family. Indeed, when one superimposes on a helical wheel the TM11 sequences of Ste6, CepgpC, Mdr65, Pfmdr1, Cftr, and Atpgp, it is noticeable that the mutation-neutral hydrophobic face of the helix is more sequence-variable than the mutation-sensitive hydrophilic face (data not shown). This pattern of conservation has been described in other families of membrane transporters (Baldwin, 1993; Donnelly & Cogdell, 1993; Donnelly *et al.*, 1993). Taken together, these findings suggest a model for TM11 in which the most hydrophobic face of the helix would interact with lipid molecules in the

Gene	TM	TM Domain	Reference
mouse mdr3 - 11	mKKAh	VFGItFsftqAmYFSYAacF	RFGayLVt M33581
mouse mdr2 - 11	VrKAh	IYGI tFsIsqaFmYFSYAacF	RFGsyLIV J03398
mouse mdr1 - 11	mKKAh	VFGItFsftqAmYFSYAacF	RFGayLva M14757
hamster pgp1 - 11	lKKAh	VFGItFsftqAmYFSYAacF	RFGayLva M59253
hamster pgp2 - 11	lKKAh	VFGItFsftqAmYFSYAacF	RFGayLva M60041
hamster pgp3 - 11	VqmAh	IYGI tFsIsqaFmYFSYAacF	RFGayLIV M60042
rat mdr1 - 11	lKKAh	VFGItFaftqAmYFSYAacF	RFGayLva JH0502
rat mdr2 - 11	VrKAh	IYGI tFsIsqaFmYFSYAacF	RFGsyLIV L15079
human mdr1 - 11	lrKAh	IFGI tFsftqAmYFSYAacF	RFGayLva M14758
human mdr3 - 11	VQKAh	IYGI tFsIsqaFmYFSYAacF	RFGayLIV M23234
mouse mdr1 - 5	IKKAI	tasISigIAYLLVYaSYALaF	WYGtsLVl M14757
mouse mdr2 - 5	IKKAI	sanISmgIAFLLIYaSYALaF	WYGstLVI J03398
mouse mdr3 - 5	IKKAI	tanISmgAFLLIYaSYALaF	WYGtsLVI M33581
hamster pgp1 - 5	IKKAI	tanISmgAFLLIYaSYALaF	WYGtsLVI M59253
hamster pgp2 - 5	IKKAV	tanISigIAYLLVYaSYALaF	WYGtsLVl M60041
hamster pgp3 - 5	IKKAI	sanISmgIAFLLIYaSYALaF	WYGstLVI M60042
rat mdr1 - 5	IKKAI	tanISigIAYLLVYaSYALaF	WYGtsLVl JH0502
rat mdr2 - 5	IKKAI	sanISmgIAFLLIYaSYALaF	WYGstLVI L15079
human mdr1 - 5	IKKAI	tanISigAFLLIYaSYALaF	WYGtsLVl M14758
human mdr3 - 5	IKKAI	sanISmgIAFLLIYaSYALaF	WYGstLVI M23234
human cftr - 11	lylst	lrwfgmrIemiFViFfiAvtF	isilttge M55131
mouse cftr - 11	mylat	lrwfgmrIdmiFVLffivvtF	isilttge M69298
X. laevis cftr - 11	lylst	lrwfgmtIemiFViFfiAvsF	isiatsga X65256
dogfish cftr - 11	lylst	lrwfgmrIdivFVLffivvtF	iaiatdV M83785
C. elegans pgpA - 11	IKeAf	IGLSYgcAssvlyLlntcAY	RmGlaLII X65054
C. elegans pgpC - 11	Ivrgl	wqslSFalAgSFVmWnFAlaY	mFGLwLIs X65055
S. cerevisiae ste6 - 11	raiAt	gFGISmtnmivMcicaiiyyY	--GlKLVm X15428
C. albicans hst - 11	VyrAl	qtGIGFaIsdLFssigqAilL	FYGmkLIs pers.comm.
D. melanogaster mdr49 - 11	rrKvr	frGlVfalgqaapFLaYgism	YYGgiLva M59076
D. melanogaster mdr50 - 11	krnth	frGlVYglArslmFFaYAacm	YYGtwcVI L07065
D. melanogaster mdr65 - 11	rqKlr	wrGVlnstmqasaFFaYAvAL	cYGGvLVs M59077
P. falciparum mdr - 11	krriI	VnaalWgfsqsaqLFinsfAY	WFGsfLIk M29154
A. thaliana pgp - 11	fwKgg	IaGsgYgVAqFclYaSYAlgL	WyaswLVk A42150
L. tarentolae pgpA - 11	mqnvs	nrlwlgvrleFLscvvtFmvaF	igvigkme X17154
C. elegans pgpA - 5	VlKgl	fLGISFgamqasnFiSFALaF	YiGvgWVh X65054
C. elegans pgpC - 5	IrKAI	ILaIctafpLMLMftcmAvAF	WYGatLaa X65055
S. cerevisiae ste6 - 5	IKscf	fvaanagIlrFLtLtmFvqgF	WFGsamIk X15428
C. albicans hst - 5	yKlsh	avaantaVlktLtLmmFvqgF	WFGnyLls pers.comm.
D. melanogaster mdr49 - 5	rKKgl	ysGmgnaIsWliIYLcmAlaI	WYGvtLIl M59076
D. melanogaster mdr65 - 5	qWKga	fsGLSdaVlksMlYLScaGAF	WYGvnLII M59077
P. falciparum mdr - 5	lKanf	VealhiglingLILvSYAfgF	WYGtriII M29154
E. coli hlyB	fkvtV	latIggqggliqlqktvminL	WLGahLVI M81823
P. haemolytica lktB	frvtV	latIggqggvqliqktvminL	WLGahLVI L12148
E. coli cvaB	IKltr	mdllfggIntFvtacdqiViL	WLGagLVI X57524
R. meliloti ndvA	ypvld	wWalasglNriastiSmmail	viGtvLVq M20726
A. tumefaciens chvA	ypvld	wWafasalnrstastvSmmiiL	viGtvLVk M24198

FIGURE 7: Alignment of predicted TM5 and TM11 sequences from known P-glycoproteins and other eukaryotic and prokaryotic members of the ABC superfamily of transporters. Reference indicates the Genbank accession number of each sequence. The reference of the *Candida albicans* HST homolog is a personal communication from Dr. M. Raymond. Arrows point to position of Y949 and F953 in mouse Mdr3.

membrane bilayer, and that this interaction would tolerate substitutions to the neutral amino acid alanine. On the other hand, the more hydrophilic and mutation-sensitive face of the TM11 helix may be involved in interactions between TM11 and other TM helices of P-gp, or alternatively may contact directly substrate molecules. Both types of interaction would be important for determining the overall specificity of P-gp, and perhaps also of other ABC transporters. Finally, we observed a loose gradation of the severity of the deleterious effect of mutations increasing from the direction of the presumed cytoplasmic (inner lipid leaflet) to the extracellular (outer leaflet) end of TM11. This is evident in the helical wheel projection of TM11 (Figure 4) in which one face of the helical stack shows a gradient of mutation severity, ranging from essentially none (G935A) at the cytoplasmic end to the most severe mutation being in the last residue of TM11 before the extracellular loop (F953A). These results suggest that the outer portion of TM11 and perhaps the following extracellular loop play a particularly important role in substrate recognition. This conclusion is

in good agreement with the recent analysis of the drug resistance profiles and photolabeling characteristics of chimeric and mutant human MDR1 P-gps altered in the TM11/TM12 region, which also suggested a similar important functional role for this region of the protein (Zhang *et al.*, 1995).

Pawagi *et al.* (1994) have analyzed computer predictions of the α -helical structure of the 12 TM domains of P-gp and modeled potential interactions between the TM domains and a typical hydrophobic cationic substrate (rhodamine 123). On the basis of the high proportion of amino acids with aromatic side chains detected in the TM domains of P-gp, they have proposed that the spatial distribution of aromatic rings (e.g., F and Y residues) may allow for intercalation of drug molecules, possibly resulting in the formation of a "transport path" involving interactions with the π electron rings of some of the drug molecules. This transport path could be either in a protein/lipid interface or in an internal "pore" formed by several helices coming together. Our observations that the two most severe mutations in TM11

are in two aromatic amino acids is in agreement with the model proposed by Pawagi *et al.* and suggests that these residues may be involved in such aromatic ring hydrophobic interactions.

F953A was the most deleterious mutation of the 21 mutations analyzed in our study, causing a 2 \times , 6 \times , 10 \times , and 10 \times reduction in resistance to VBL, ACT, COL, and ADR, respectively, relative to WT Mdr3. In previous work (Loo & Clarke, 1993b), the same mutation was made in the same residue at the equivalent position in P-gp encoded by the human *MDR1* isoform (F957A). In these studies, the individual substitutions of five TM11 phenylalanine residues to alanines were without consequence on P-gp activity. Since the human and mouse TM11 sequences are identical, the difference in the behavior of our mutant and that of Loo and Clarke at the same position was surprising. To test the possibility that unwanted mutations outside F953A may have been picked up during the construction of this clone and may be responsible for the altered phenotype of our mutant, we repeated in its entirety the construction of the F953A mutant and retested its activity in transfected cells. Results obtained with this second construct were identical to those shown in this paper (data not shown). In addition, immunofluorescence experiments indicated similar overall levels of expression and similar patterns of subcellular distribution of wild-type and F953A proteins (typical of membrane-associated expression) in transfected CHO cells (Figure 5). Finally, we expressed wild-type Mdr3 and the F953A mutant in yeast cells and compared their biological activity. We have recently established that mouse Mdr3 is functional in yeast and can complement the biological activity of the endogenous yeast pheromone transporter Ste6 and restore mating in an otherwise sterile *ste6* mutant (Raymond *et al.*, 1992), but it can also confer cellular resistance to the antifungal agent FK506 (Raymond *et al.*, 1994) and the peptide ionophore valinomycin (Kuchler & Thorner, 1992). Yeast cells were transformed with expression vectors carrying either wild-type *mdr3* or mutant *F953A mdr3* cDNAs, followed by selection for *ura*⁺ cells, and the level of expression of the two proteins in highly enriched membrane fractions from these cells was analyzed using the anti-Mdr3 antibody B2037. This antibody detected strong and comparable expression of the two proteins in these membrane fractions (Figure 8A). We then monitored the effect of Mdr3 and F953A expression (two mass populations for the latter) on cellular resistance to the fungicidal agents and Mdr3 substrates in yeast, FK506 (Figure 8B) and valinomycin (Figure 8C), using a growth inhibition assay in liquid cultures (Raymond *et al.*, 1994). We observed that Mdr3 could confer resistance and allow growth of yeast cells in medium containing either FK506 and valinomycin. In contrast, the F953A mutation was found to abrogate resistance to FK506, while it had no effect on the capacity of Mdr3 to convey resistance to valinomycin. These results indicate that the F953A mutation is unlikely to cause gross alterations impairing membrane targeting or insertion but rather is likely to affect substrate specificity. Therefore, studies in yeast are in full agreement with the previous characterization of these proteins in CHO cells. Differences in the expression system and cell lines used by our group to study the mouse F953A Mdr3 mutant and those used by Loo and Clarke to study the homologous human *MDR1* mutant may contribute to the observed differences in activity. Finally, although mouse Mdr3 and human *MDR1* share up to 90% amino acid

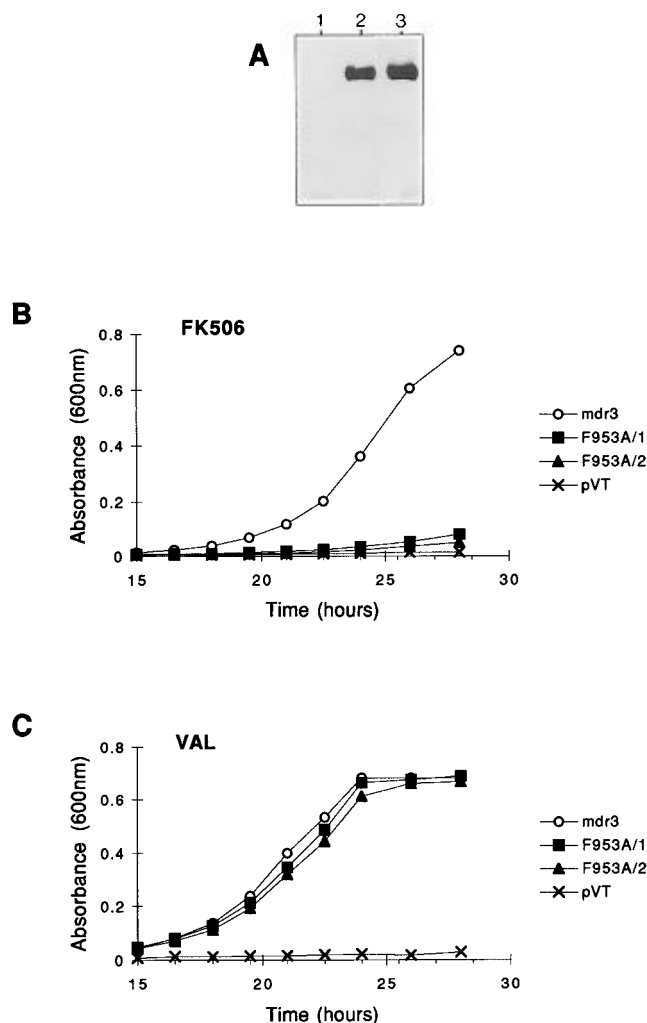


FIGURE 8: Expression of wild-type Mdr3 and mutant F953A in yeast cells. (A) JPY201 yeast cells were transformed with either control pVT plasmid (pVT) or pVT-*mdr3* (*mdr3*) or pVT-*mdr3F953A* expression plasmids, and enriched membrane fractions were prepared from pVT (1), pVT-*mdr3* (2), or pVT-*mdr3F953A* (3) transformants and analyzed for the presence of the corresponding Mdr3 protein by immunoblotting using the rabbit anti-mouse Mdr3 antibody B2037. Yeast transformants harboring control pVT, control pVT-*mdr3*, or the *F953A* mutant (two mass populations for F953A, F953A/1 and F953A/2) were seeded in 96-well plates containing either FK506 (B) or valinomycin (C) at 50 μ g/mL, as described in Materials and Methods. Growth was measured by optical density at 490 nm and was monitored over a 28-h period.

sequence similarity, they are functionally different with respect to substrate specificity and sensitivity to inhibitors (Tang-Wai *et al.*, 1995). Therefore, it is possible that mutations at the same site may affect in a different fashion transport of the same substrates in the two proteins. Further experiments are required to clarify this point.

In conclusion, our experimental results from TM11 mutagenesis by alanine scanning identify this domain as an important structural or functional determinant for drug transport by P-gp, most likely through the formation of a drug binding site. The analysis of the results with respect to a possible amphipathic character of this domain, and conservation of its amino acids in other members of the P-gp and ABC families, together suggest that residues on the more hydrophilic side of the TM11 helix play a key role in these proteins. Finally, our results should help in the determination of the secondary and tertiary structure of this domain with respect to the other TM helices and the lipid bilayer.

ACKNOWLEDGMENT

We thank Dr. R. Kaufman for the gift of plasmid pEMC2b, Dr. M. Raymond for sharing results before publication, and Dr. Danny Kaplan for producing Figure 4.

REFERENCES

- Baldwin, J. M. (1993) *EMBO J.* 12, 1693–1703.
- Bruggemann, E. P., Germann, U. A., Gottesman, M. M., & Pastan, I. (1989) *J. Biol. Chem.* 264, 15483–15488.
- Bruggemann, E. P., Currier, S. J., Gottesman, M. M., & Pastan, I. (1992) *J. Biol. Chem.* 267, 21020–21026.
- Buschman, E., & Gros, P. (1991) *Mol. Cell. Biol.* 11, 595–603.
- Chen, C.-j., Chin, J. E., Ueda, K., Clark, D. P., Pastan, I., Gottesman, M. M., & Roninson, I. B. (1986) *Cell* 47, 381–389.
- Choi, K., Chen, C.-j., Kriegler, M., & Roninson, I. B. (1988) *Cell* 53, 519–529.
- Cornwell, M. M., Safa, A. R., Felsted, R. L., Gottesman, M. M., & Pastan, I. (1986) *Proc. Natl. Acad. Sci. U.S.A.* 83, 3847–3850.
- Cornwell, M. M., Tsuruo, T., Gottesman, M. M., & Pastan, I. (1987) *FASEB J.* 1, 51–54.
- Devault, A., & Gros, P. (1990) *Mol. Cell. Biol.* 10, 1652–1663.
- Devereux, J. (1991) The GCG sequence analysis software package, version 7.0, Genetics Computer Group, Inc., University Research Park, Madison, WI.
- Devine, S. E., Ling, V., & Melera, P. W. (1992) *Proc. Natl. Acad. Sci. U.S.A.* 89, 4564–4568.
- Dhir, R., & Gros, P. (1992) *Biochemistry* 31, 6103–6110.
- Dhir, R., Grizzuti, K., Kajiji, S., & Gros, P. (1993) *Biochemistry* 32, 9492–9499.
- Donnelly, D., & Cogdell, R. J. (1993) *Protein Eng.* 6, 629–635.
- Donnelly, D., Overington, L. P., Ruffle, S. V., Nugent, J. H. A., & Blundell, T. L. (1993) *Protein Sci.* 2, 55–70.
- Endicott, J. A., & Ling, V. (1989) *Annu. Rev. Biochem.* 58, 137–171.
- Foote, S. J., Kyle, D. E., Martin, R. K., Oduola, A. M. J., Forsyth, K., Kemp, D. J., & Cowman, A. F. (1990) *Nature* 345, 255–258.
- Gottesman, M. M., & Pastan, I. (1993) *Annu. Rev. Biochem.* 62, 385–427.
- Greenberger, L. M. (1993) *J. Biol. Chem.* 268, 11417–11425.
- Greenberger, L. M., Lisanti, C. J., Silva, J. T., & Horwitz, S. B. (1991) *J. Biol. Chem.* 266, 20744–20751.
- Gros, P., Croop, J., & Housman, D. (1986) *Cell* 47, 371–380.
- Gros, P., Raymond, M., Bell, J., & Housman, D. (1988) *Mol. Cell. Biol.* 8, 2770–2778.
- Gros, P., Dhir, R., Croop, J., & Talbot, F. (1991) *Proc. Natl. Acad. Sci. U.S.A.* 88, 7289–7293.
- Higgins, C. F. (1992) *Annu. Rev. Cell Biol.* 8, 67–113.
- Ito, H., Fokuda, K., Murata, K., & Kimura, A. (1983) *J. Bacteriol.* 153, 163–168.
- Kajiji, S., Talbot, F., Grizzuti, K., Van Dyke-Phillips, V., Agresti, M., Safa, A. R., & Gros, P. (1993) *Biochemistry* 32, 4185–4194.
- Kajiji, S., Dreslin, J. A., Grizzuti, K., & Gros, P. (1994) *Biochemistry* 33, 5041–5048.
- Kartner, N., Evernden-Porcelle, D., Bradley, G., & Ling, V. (1985) *Nature* 316, 820–823.
- Kuchler, K., & Thorner, J. (1992) *Proc. Natl. Acad. Sci. U.S.A.* 89, 2302–2306.
- Laemmli, U. K. (1970) *Nature* 227, 680–685.
- Loo, T. W., & Clarke, D. M. (1993a) *J. Biol. Chem.* 268, 3143–3149.
- Loo, T. W., & Clarke, D. M. (1993b) *J. Biol. Chem.* 268, 19965–19972.
- Loo, T. W., & Clarke, D. M. (1994a) *J. Biol. Chem.* 269, 7243–7248.
- Loo, T. W., & Clarke, D. M. (1994b) *Biochemistry* 33, 14049–14057.
- McGrath, J. P., & Varshavsky, A. (1989) *Nature* 340, 400–404.
- Morris, D. I., Speicher, L. A., Ruoho, A. E., Tew, K. D., & Seamon, K. B. (1991) *Biochemistry* 30, 8371–8379.
- Morris, D. I., Greenberger, L. M., Bruggemann, E. P., Cardarelli, C., Gottesman, M. M., Pastan, I., & Seamon, K. B. (1994) *Mol. Pharmacol.* 46, 329–337.
- Pawagi, A. B., Wang, J., Silverman, M., Reithmeier, R. A. F., & Deber, C. M. (1994) *J. Mol. Biol.* 235, 554–564.
- Pollard, J. W., & Stanners, C. P. (1979) *J. Cell Physiol.* 98, 571–585.
- Raviv, Y., Pollard, H. B., Bruggemann, E. P., Pastan, I., & Gottesman, M. M. (1990) *J. Biol. Chem.* 265, 3975–3980.
- Raymond, M., Gros, P., Whiteway, M., & Thomas, D. Y. (1992) *Science* 256, 232–234.
- Raymond, M., Ruetz, S., Thomas, D. Y., & Gros, P. (1994) *Mol. Cell. Biol.* 14, 277–286.
- Ruetz, S., & Gros, P. (1994a) *J. Biol. Chem.* 269, 12277–12284.
- Ruetz, S., & Gros, P. (1994b) *Cell* 77, 1071–1081.
- Ruetz, S., Raymond, M., & Gros, P. (1993) *Proc. Natl. Acad. Sci. U.S.A.* 90, 11588–11592.
- Safa, A. R., Glover, C. J., Meyers, M. B., Biedler, J. L., & Felsted, R. L. (1986) *J. Biol. Chem.* 261, 6137–6140.
- Safa, A. R., Metha, N. D., & Agresti, M. (1989) *Biochem. Biophys. Res. Commun.* 162, 1402–1408.
- Safa, A. R., Stern, R. K., Choi, K., Agresti, M., Tamai, I., Mehta, N. D., & Roninson, I. B. (1990) *Proc. Natl. Acad. Sci. U.S.A.* 87, 7225–7229.
- Sanger, F., Nicklen, S., & Coulson, A. R. (1977) *Proc. Natl. Acad. Sci. U.S.A.* 74, 5463–5467.
- Schinkel, A. H., Roelofs, M. E. M., & Borst, P. (1991) *Cancer Res.* 51, 2628–2635.
- Schinkel, A. H., Smit, J. J. M., van Tellingen, O., Beijnen, J. H., Wagenaar, E., van Deemter, L., Mol, C. A. A. M., van der Valk, M. A., Robanus-Maandag, E. C., te Riele, H. P. J., Berns, A. J. M., & Borst, P. B. (1994) *Cell* 77, 491–502.
- Schurr, E., Raymond, M., Bell, J. C., & Gros, P. (1989) *Cancer Res.* 49, 2729–2734.
- Shapiro, A. B., & Ling, V. (1994) *J. Biol. Chem.* 269, 3745–3754.
- Shustik, C., Dalton, W., & Gros, P. (1995) *Mol. Aspects Med.* 16, 1–78.
- Simon, S. M., & Schindler, M. (1994) *Proc. Natl. Acad. Sci. U.S.A.* 91, 3497–3504.
- Skehan, P., Storeng, R., Scudiero, D., Monks, A., McMahon, J., Vistica, D., Warren, J., Bokesch, H., Kenny, S., & Boyd, M. R. (1989) *Proc. Am. Assoc. Cancer Res.* 30, 612.
- Smith, A. J., Timmermans-Hereijgers, J. L. P. M., Roelofs, B., Wirtz, K. W. A., van Blitterswijk, W. J., Smit, J. J. M., Schinkel, A. H., & Borst, P. (1994) *FEBS Lett.* 354, 263–266.
- Southern, P. J., & Berg, P. (1982) *J. Mol. Appl. Genet.* 1, 327–341.
- Tang-Wai, D. F., Bossi, A., Arnold, L. D., & Gros, P. (1993) *Biochemistry* 32, 6470–6476.
- Tang-Wai, D. F., Kajiji, S., DiCapua, F., de Graaf, D., Roninson, I. B., & Gros, P. (1995) *Biochemistry* 34, 32–39.
- van der Blik, A. M., Kooiman, P. M., Schneider, C., & Borst, P. (1988) *Gene* 71, 401–411.
- Wigler, M., Pellicer, A., Silverman, S., Axel, R., Urlaub, G., & Chasin, L. (1979) *Proc. Natl. Acad. Sci. U.S.A.* 76, 1373–1376.
- Zhang, X., Collins, K., & Greenberger, L. M. (1995) *J. Biol. Chem.* 270, 5441–5448.

BI951333P